Title
BCL6 Antagonizes NOTCH2 to Maintain Survival of Human Follicular Lymphoma Cells

Journal
Cancer Discovery, 7(5)

ISSN
2159-8274

Authors
Valls, Ester
Lobry, Camille
Geng, Huimin
et al.

Publication Date
2017-05-01

DOI
10.1158/2159-8290.cd-16-1189

Peer reviewed

Published in final edited form as:

Cancer Discov. 2017 May ; 7(5): 506–521. doi:10.1158/2159-8290.CD-16-1189.

BCL6 antagonizes NOTCH2 to maintain survival of human follicular lymphoma cells

Ester Valls[1,#], **Camille Lobry**[2,7,#], **Huimin Geng**[1,3,8], **Ling Wang**[1], **Mariano Cardenas**[1], **Martín Rivas**[1], **Leandro Cerchietti**[1], **Philmo Oh**[2], **Shao Ning Yang**[1], **Erin Oswald**[1], **Camille W. Graham**[4], **Yanwen Jiang**[1], **Katerina Hatzi**[1,9], **Xabier Agirre**[1,10], **Eric Perkey**[5,11], **Zhuoning Li**[1], **Wayne Tam**[6], **Kamala Bhatt**[2], **John P. Leonard**[1], **Patrick A. Zweidler-McKay**[4], **Ivan Maillard**[5], **Olivier Elemento**[3], **Weimin Ci**[1,12,*], **Iannis Aifantis**[2,*], and **Ari Melnick**[1,*]

[1]Division of Hematology/Oncology, Department of Medicine; Weill Cornell Medical College, New York, NY, 10065, USA

[2]Department of Pathology and Perlmutter Cancer Center, New York University School of Medicine, New York, New York 10016, USA

[3]Institute for Computational Biomedicine, Weill Cornell Medical College, New York, NY, 10065, USA

[4]Division of Pediatrics, University of Texas M. D. Anderson Cancer Center, Houston, TX 77030, USA

[5]Life Sciences Institute, Division of Hematology-Oncology, Department of Internal Medicine; University of Michigan, Ann Arbor, MI, USA

[6]Department of Pathology and Laboratory Medicine, Weill Cornell Medical College, New York, NY, 10065, USA

[7]Institut Gustave Roussy, INSERM U1170, Villejuif and Université Paris Sud, Orsay, France

[8]Department of laboratory Medicine, University of California San Francisco, San Francisco, CA, 94143, USA

[9]Department of Cancer Biology and Genetics, Memorial Sloan Kettering Cancer Center, New York, New York 10065, USA

[10]Division of Hematology/Oncology, Centre for Applied Medical Research (CIMA), University of Navarra, Pamplona, Spain

[11]Graduate Program in Cellular and Molecular Biology

[*]To whom Correspondence should be addressed: Ari Melnick, MD, Division of Hematology/Oncology, Department of Medicine, Weill Cornell Medical College, 413 East 69th Street, BB-1462, New York, NY 10021, T: +1 646-962-7502; amm2014@med.cornell.edu; Iannis Aifantis, PhD, Department of Pathology and Perlmutter Cancer Center, New York University School of Medicine, 552 1st Ave, SBR 1304, New York 10016, NY, USA, T: +1 212 263 9898; iannis.aifantis@nyumc.org; Weimin Ci, PhD, Beijing Institute of Genomics, Chinese Academy of Sciences, No.1 Beichen West Road, Chaoyang District, Beijing, China, 100101, T: +86-10-840973318; ciwm@big.ac.cn.

[#]EV and CL contributed equally to this work.

Conflict of Interest. The authors do not have any conflicts of interest pertinent to this research.

[12]Key Laboratory of Genomic and Precision Medicine, Beijing Institute of Genomics, Chinese Academy of Sciences, Beijing, 100101, China

Summary

Although the BCL6 transcriptional repressor is frequently expressed in human follicular lymphomas (FL), its biological role in this disease remains unknown. Herein we comprehensively identify the set of gene promoters directly targeted by BCL6 in primary human FLs. We noted that BCL6 binds and represses *NOTCH2* and Notch pathway genes. Moreover, *BCL6* and *NOTCH2* pathway gene expression is inversely correlated in FL. Notably BCL6 up-regulation is associated with repression of Notch2 and its target genes in primary human and murine germinal center cells. Repression of Notch2 is an essential function of BCL6 in FL and GC B-cells since inducible expression of *Notch2* abrogated GC formation in mice and kills FL cells. Indeed BCL6-targeting compounds or gene silencing leads to the induction of NOTCH2 activity and compromises survival of FL cells whereas *NOTCH2* depletion or pathway antagonists rescue FL cells from such effects. Moreover, BCL6 inhibitors induced NOTCH2 expression and suppressed growth of human FL xenografts *in vivo* and primary human FL specimens *ex vivo*. These studies suggest that established FLs are thus dependent on BCL6 through its suppression of *NOTCH2*.

Keywords

Follicular lymphoma; Germinal center reaction; Transcriptional repression; BCL6; Transcription factor targeted therapy

Introduction

Follicular lymphoma (FL) is the second most common form of non-Hodgkin lymphoma (1). It is generally an indolent and slow growing disease that is nonetheless mostly incurable with currently available chemo-immunotherapy regimens (1). FLs arise from germinal center (GC) B-cells. GCs are transient structures that develop after exposure to T-cell dependent antigen. To form GCs B-cells aggregate within lymphoid follicles and initiate a program of rapid proliferation and somatic hypermutation of their immunoglobulin loci for the purpose of generating high affinity antibodies. These rapidly proliferating B-cells are called centroblasts and are dependent on the presence of the transcriptional repressor BCL6, which is a master regulator of the GC reaction. As clones of B-cells emerge within the GC they encounter T-cells and follicular dendritic cells. Signaling events that ensue select B-cells with high affinity antibody for terminal differentiation into memory and B-cells. During this signaling process the B-cells slow down and adopt an intermediate state between pre- and post-GC phenotypes where they are called centrocytes. FL phenotype and gene expression profiles reflect aspects of centroblasts and centrocytes of the GC reaction.

From the molecular standpoint, FLs almost universally harbor t(14;18) translocations involving fusion of *BCL2* to regulatory elements associated with immunoglobulin heavy chain locus (2). Constitutive expression of *BCL2* suppresses apoptosis, which would otherwise occur physiologically in GC B-cells. Mice engineered to express *BCL2* under the control of the VAV2 promoter develop a FL-like disease, albeit with a long latency period

(3). BCL2 is a direct transcriptional target of BCL6, which causes its expression to be completely silenced during the GC reaction. Translocation of BCL2 enables its escape from BCL6 repression. This leads to a situation where both proteins BCL2 and BCL6 are expressed together. Along these lines, it has been reported that >90% of FL cases express BCL6 (4,5). The implication of BCL6 expression in FL has not been explored.

In normal GC B-cells the most established function of BCL6 is to repress critical checkpoint and DNA damage repair pathway genes including *ATR, CHEK1, TP53, CDKN1A*, etc. Through this mechanism GC B-cells can proliferate and tolerate the DNA damage associated with somatic hypermutation and class switch recombination (6). The survival and growth checkpoint functions of BCL6 are also maintained in diffuse large B-cell lymphomas (DLBCLs), which like FL derive from GC B-cells. BCL6 expression in DLBCL is maintained in part through chromosomal translocations, although most DLBCLs express BCL6 regardless of genetic lesions. Functional assays demonstrate that DLBCL cells are dependent on BCL6 regardless of translocations (6). Hence BCL6 more than an oncogene is actually a lineage factor for DLBCL. BCL6 is a member of the BTB-POZ family of transcription factors, and mediates transcriptional repression in large part by recruiting the SMRT, NCoR and BCoR corepressors via the BTB domain (6). Specific peptidomimetic inhibitors of the BCL6 BTB domain kill DLBCL cells *in vitro* and *in vivo* (7–9).

Traditionally BCL6 has not been considered as a phenotypic driver in FL, since these tumors, particularly the low grade ones only rarely display BCL6 translocations in their early stages, and have an indolent phenotype. However, the potent oncogenic functions of BCL6 make it unlikely that its constitutive expression in FL is merely a passenger marker. BCL6 biological functions are dependent on the target genes that it regulates. The biological functions of BCL6 are not likely limited to repressing cell growth and DNA damage checkpoints. It is entirely possible that other sets of target genes might be crucial for putative roles of BCL6 in FL. Indeed previous work showed that BCL6 may function through partially different target genes in DLBCL as compared to normal GC B-cells (10). Based on these considerations we hypothesized that BCL6 might also function as an oncoprotein in FL and that any such role would be linked to repression of specific sets of target genes. Discovery of BCL6 target genes in FL seemed like an appropriate starting point to address these questions. Through this approach we report a novel function for BCL6 in binding and repressing expression and activity of NOTCH2 in FL cells. Repression of NOTCH2 by BCL6 is required to maintain the survival of FL cells. We show that this function is inherited from GC B-cells and is required for development of GCs during the humoral immune response. Finally, we find that BCL6 targeted therapy potently kills FL derived cell lines both *in vitro* and *in vivo*, and most importantly, also kills primary human FL patient specimens *ex vivo*.

Results

BCL6 regulates specific genes and pathways in FL including NOTCH2

As a first approach to exploring BCL6 functions in FL we performed ChIP-on-chip to identify direct target genes relevant to this disease. Since no cell lines are available that reflect FL biology in its indolent phase, we performed these studies using CD20 purified B-

cells from four independent primary FL patient samples with >80% tumor cell content. ChIP products were co-hybridized with their respective inputs to microarrays representing 25,000 promoters. BCL6 binding sites were identified by random permutation analysis and a peak overlap algorithm (10). 48.4% of BCL6 binding sites overlapped between the four FL specimens, amounting to a total of 1529 probesets and corresponding to 1712 genes (Supplementary Table S1). DNA motif analysis confirmed that BCL6 canonical DNA binding sequence was highly enriched at these BCL6 binding sites ($p<1.7^{-7}$, FIRE algorithm with hypergeometric test (11), data not shown). To determine whether BCL6 targets in FL lymphoma cells were associated with particular biological functions we queried curated gene signatures relevant to lymphomagenesis (12). The top 5 gene sets captured by this method using Fisher's exact tests with Benjamini-Hochberg (BH) correction included known direct BCL6 targets from experiments in the Ramos cell line (9), a DLBCL proliferation signature (13), a cell cycle gene set (14), a Notch induced gene signature (15) and genes repressed by Blimp1 (16) (Fig. 1A, Supplementary Table S2). We noted that repression of Notch was not a previously recognized function of BCL6 in the context of B-cell lymphomas.

To distinguish BCL6 target genes likely to contribute to the FL phenotype, we sought to identify those targets most strongly repressed in FL. Analysis of gene expression profiles from 191 FL patients (17) demonstrated that 184 FL BCL6 target genes displayed significant inverse correlation with BCL6 expression, including NOTCH2 (Spearman correlation, $p<0.05$, Fig. 1B and Supplementary Table S3). To determine whether these 184 genes were enriched for any particular pathway category we explored their functional annotation using DAVID (Supplementary Fig. S1A). This analysis again highlighted NOTCH2 as well as Notch pathway genes involved in cell cycle, apoptosis, cellular morphogenesis, lymphoid organ development or transcription (Supplementary Fig. S1B). These data suggested that BCL6 might be a repressor of NOTCH2 and NOTCH signaling pathways. In further support of this notion we observed inverse correlation between expression of BCL6 and expression of a curated list (15,18,19) of NOTCH cofactors and target genes among which *NOTCH2* was the most inversely correlated (Spearman correlation, $p<0.05$, Fig. 1C and Supplementary Table S4). Examination of BCL6 read densities at the NOTCH2 promoter in the 4 FL specimens showed enrichment as compared to negative control genes (HPRT and COX6B, Fig. 1D and Supplementary Fig. S1C), similar in magnitude to its enrichment at canonical BCL6 targets like TP53 and BCL6 itself (Fig. S1C). Moreover, we identified canonical BCL6 DNA binding sites in the regulatory regions of the Notch cofactor genes *MAML1*, *MAML2* and *RBP-Jk*, all members of the Notch co-activator complex, as well as *HES1* a transcriptional repressor and the prototypic Notch pathway transcriptional target (Fig. 1E). To validate whether these are true BCL6 targets we performed QChIP and confirmed that BCL6 is indeed bound to these loci in two independent FL derived cell lines (Fig. 1F). Primers used to this analysis are found at Supplementary Table S5.

Since GC B-cells are the cell of origin of FL, and FL gene expression profiles reflect GC B-cell transcriptional programming we wondered if BCL6 could bind to the Notch2 locus in this setting as well. Binding of BCL6 to the promoters of NOTCH2, MAML2 and RBP-Jk was confirmed by performing QChIP in independent primary human GC B-cells

(Supplementary Fig. S1D). In addition to FL, GC B-cells give rise to DLBCLs. To determine whether BCL6 could bind and regulate Notch2 and related genes in DLBCLs we used BCL6 ChIp-on chip data performed and analyzed on the same platform as the FLs (10). Among BCL6 target genes in DLBCL cells the Notch induced gene signature was not significantly enriched (Supplementary Table S6, S7 and S8) although other gene sets overrepresented in FL BCL6 target genes were also enriched in DLBCL (Supplementary Fig. S1E and Supplementary Table S6). Analysis of gene expression profiles from 71 DLBCL patient samples(20) showed that 245 DLBCL BCL6 target genes displayed significant inverse correlation with BCL6 expression (Spearman correlation, $p<0.05$, Supplementary Table S7). Nonetheless, analysis of the curated list of NOTCH cofactors and target genes from Figure 1C indicated that *NOTCH2* and other Notch pathway partners were inversely correlated (Spearman correlation, $p<0.05$, Supplementary Fig. S1G and Supplementary Table S8). Furthermore, less than 15% of the genes found in DLBCL subset were shared with the ones found on FL subset (Spearman correlation, $p<0.05$, Supplementary Table S9). Altogether these results point to NOTCH2 and its cofactors as *bona fide* BCL6 target genes with potential relevance to the phenotype of FL tumors as well as formation of GCs during the humoral immune response. Although repression of Notch pathway is not as strongly linked with DLBCL, it is evident that BCL6 represses NOTCH2 in this disease subtype as well.

BCL6 and NOTCH2 are inversely correlated in GC B-cells

Upregulation of BCL6 is required for mature follicular B-cells to differentiate into GC B-cells during the humoral immune response. In contrast NOTCH2 plays a critical role in marginal zone differentiation, which is an alternative cell fate for follicular B-cells (21). Hence we wondered whether upregulation of BCL6 in human GC B-cells would be associated with silencing of *NOTCH2.* We purified primary human naïve B-cells (NB) and GC B-cells from human tonsils, and confirmed their purity by IgD^+ and $CD38^+$ staining respectively (Supplementary Fig. S2A). We then measured the relative transcript abundance of *NOTCH2, MAML1* and *MAML2* as well as *BCL6* by QPCR (Fig. 2A). While *BCL6* was upregulated in GC B-cells, *NOTCH2, MAML1* and *MAML2* (but not *RBP-Jk*) were concordantly downregulated (Fig. 2A). Examination of available gene expression profiles obtained from five independent sets of NB and GC B-cells (22) confirmed downregulation of *NOTCH2, MAML1* and Notch target genes in GC B-cells and the inverse correlation with *BCL6* (Fig. 2B and Supplementary Table S10; probesets for *MAML2* were not present on this array). Notch2 protein downregulation in GC B-cells was further confirmed by immunoblotting (Supplementary Fig. S2B). During the GC reaction B-cells first become proliferative centroblasts (CB) and then become centrocytes (CC) as they interact with T cells in the GC light zone. We analyzed gene expression in these cell types using RNA-seq, and again observed inverse correlation between BCL6 and NOTCH2 in both CB and CC (Figs. 2C–D).

In order to determine whether these changes in gene expression are linked to GC activation signals, we purified human and murine mature B-cells, independently co-cultured them with stromal cells (OP9) and exposed them to IL4 and IL21 (23,24). Murine mature B-cell purity was confirmed by $CD45/B220^+$ staining by flow cytometry (Supplementary Fig. S2C). In

both human and murine cells we observed significant BCL6 upregulation ($p<0.0001$; $p=0.0004$ human and murine cells respectively) associated with downregulation of *NOTCH2* ($p=0.0136$; $p=0.044$) and *MAML2* ($p=0.0029$; $p=0.0255$), although expression of *MAML1* ($p=0.1069$; $p=0.0609$) and *RBP-Jk* ($p=0.0784$; $p=0.1841$) was more variable (Fig. 2E–F). These data suggest that BCL6 repression of *NOTCH2* is an integral feature of normal GC B-cell activation and may be critical to specifying the GC phenotype in opposition to marginal zone differentiation.

NOTCH2 expression impairs GC formation

Given that BCL6 is required for development of GC formation and directly represses NOTCH2, we wondered whether expression of an active form of NOTCH2 (intracellular domain, ICN2) in GC B-cells might disrupt GC formation. To address this question we studied GC formation in a mouse strain engineered to contain an ICN2-IRES-YFP (ICN2) cassette with a loxP flanked start site knocked-in to the ROSA26 locus(25). These mice were crossed with a tamoxifen inducible ROSA26-Cre-ER^{T2} strain or in ROSA26-WT control mice. GC formation was induced by immunization with the T-cell dependent antigen NP_{65}-CGG. ICN2 expression was induced the following day by tamoxifen injection. Animals were sacrificed 14 days later and spleens resected for analysis (Supplementary Fig. S3A). Paraffin-embedded spleen sections from WT and ICN2 mice were stained for the GC specific marker PNA (peanut agglutinin), or for BCL6 and B220. GCs were defined as clusters of PNA^+ or $BCL6^+/B220^+$ cells (Fig. 3A–B). As compared to WT, ICN2 conditional mice exhibited significant reduction in PNA^+ or $BCL6^+/B220^+$ GC per spleen section (mean of 29 vs. 4, $p=0.0005$, unpaired two-tailed *t* test; and mean 22 vs. 4 $p=0.0003$, respectively, Fig. 3C–D). The average size of the GCs was also reduced by two to three fold vs. WT controls (mean of 262+/−36 vs. 91+/−10 μm^2 for PNA^+, $p=0.0015$, and 177+/−30 vs. 84+/−13 μm^2 for $BCL6^+/B220^+$, $p=0.0336$ respectively, Fig. 3E–G). A more quantitative analysis of GC B-cells was generated by flow cytometry. In the presence of ICN2, the abundance of $B220^+GL7^+CD95^+$ GC B-cells was reduced three-fold as compared to WT animals (1.7% vs. 0.6% mean GC B-cells vs. total splenocytes, $p=0.0003$ unpaired two-tailed *t* test Fig. 3H–I).

Formation of GCs requires cooperation between different cell types. Hence it is conceivable that ER-induced ICN2 impairment in GC formation could be attributed to non-B cell effects. Therefore we established a second mouse model that specifically limits conditional expression of ICN2 to GC B-cells. In this case the C1γCre mice strain, which activates Cre expression in GC B-cells(26) was crossed to ROSA26-WT or ROSA26-ICN2-IRES-YFP (from now on WT and ICN2 respectively). These animals were immunized with the T-cell dependent antigen sheep red blood cells (SRBC). Paraffin-embedded spleen sections from WT and ICN2 mice were stained for PNA, or BCL6/B220, to identify GCs (Supplementary Fig. S3B–C). These experiments again yielded significant reduction in the numbers of GCs in ICN2 conditional mice, with a mean of 13 vs. 4 PNA^+ GC per spleen section, ($p=0.0001$, unpaired two-tailed *t* test) and 14 vs. 5 $BCL6^+/B220^+$ GC per spleen, ($p=0.0001$, Supplementary Fig. S3D–E). The average size of the GCs was also significantly diminished in ICN2 expressing mice (mean of 301+/−35 vs. 68+/−17 μm^2 for PNA^+, $p<0.0001$, and 226+/−24 vs. 66+/−16 μm^2 for $BCL6^+/B220^+$, $p=0.0002$ respectively, Supplementary Fig.

S3F–H). Quantitative assessment of GC B-cells by flow cytometry yielded a three-fold reduction in the abundance of $B220^{+}GL7^{+}CD95^{+}$ GC B-cells as compared to WT animals (3.28% vs. 1.08% mean GC B-cells vs. total splenocytes, $p<0.0001$ unpaired two-tailed *t* test Supplementary Fig. S4A–B).

Consistent with the reduction in GCs (which contain cells that proliferate and undergo apoptosis) there was also reduction in the abundance of proliferating cell clusters as shown by PCNA and Ki67 immunohistochemistry (Supplementary Fig. S4C), as well as, clusters of cells with apoptotic markers caspase 3 and TUNEL in the ICN2 mice (Supplementary Fig. S4D). Given the crucial role of ICN2 in driving marginal zone B-cell differentiation we next stained for MZB markers CD21 and CD23. We observed an increase in MZB cell population in ICN2 conditional mice in detriment to Follicular B (FoB) cell population (mean of 65% +/−1.5% FoB vs. 15% +/− 2.6% MZB) compared to WT (mean of 70% +/− 3% FoB vs. 10% +/− 1.3% MZB, Supplementary Fig. S4E). In contrast as expected there was no effect on T lymphoid (single- or double-positive populations stained for CD8/CD4; top panel) or myeloid lineages (CD11b/Gr-1; bottom panel, Supplementary Fig. S4F). Altogether these data indicate that ICN2 expression is incompatible with B-cells forming GCs and that repression of *Notch2* is a critical function of BCL6 in enabling the GC phenotype.

BCL6 represses *NOTCH2* expression and activity in FL cells

To confirm that BCL6 directly represses *NOTCH2* and related genes we depleted BCL6 from FL derived cell lines using an siRNA that we validated to be specific for BCL6(27) compared to scrambled control, followed by QPCR assessment of NOTCH2, MAML1, MAML2 and RBP-Jk transcripts (Fig. 4A). We observed approximately 2-fold derepression of NOTCH2 and variable derepression of the other genes. This magnitude of derepression is similar to that reported for other BCL6 targets (7,9,10,28,29). siBCL6 was confirmed to deplete BCL6 protein (Supplementary Fig. S5A). To further confirm this result using an independent approach we treated the FL cell lines with the specific BCL6 inhibitor RI-BPI, that binds to the BCL6 BTB repression domain to block the transcriptional effects of BCL6 (7). We first validated that we could reproduce the known effect of RI-BPI in blocking the repressor activity of the BCL6 BTB domain in the context of lymphoma cell lines using a BCL6 BTB domain reporter assay (Supplementary Fig. S5B). We then measured the effect of RI-BPI on derepressing NOTCH2, MAML1, MAML2 and RBP-Jk as compared to control peptide and observed a similar effect as that seen with siRNA (Fig. 4B). There was no induction of NOTCH1, which was expressed at very low levels in these cells (data not shown). Given that NOTCH2 was also inversely correlated with BCL6 in GCB-DLBCL cells we examined the effect of RI-BPI on two such cell lines and observed generally similar degree of derepression of NOTCH2, MAML1 and MAML2 (Supplementary Fig. S5C). To determine whether upregulation of *NOTCH2* was functionally significant we performed Notch reporter assays in the FL-derived cell lines after BCL6 siRNA. BCL6 knockdown resulted in significant induction of Notch reporter activity ($p<0.0001$ in both cell lines, unpaired two-tailed *t* test), but did not affect a control reporter (Fig. 4C).

In addition to induction of expression of the NOTCH2 transcriptional complex, NOTCH activation involves signaling through NOTCH ligands (DLL1, DLL3, DLL4, JAG1, JAG2)

and cleavage by metalloproteases (ADAM10, ADAM17). To determine possible sources of NOTCH signaling in FLs and GC B-cells we measured expression of these genes in the principle FL and DLBCL cell lines used for this study (DoHH2, SC-1, OCI-Ly1 and SUD-HL-4), purified primary mature B-cell populations: NB, GC, CB, CC, MB (memory B), TPC (tonsillar plasma cell), BMPC (bone marrow plasma cell), and in a cohort of primary FL patients by RNA-seq (30,31). Expression of NOTCH ligands DLL1, DLL3, DLL4 and JAG1 was low in all of four cell lines, although JAG2 was expressed, and possibly relevant to NOTCH activation *in vitro* (Figs. 4D–E). In contrast NOTCH ligand expression was essentially absent in the relevant mature B-cell subsets, although DLL4 and JAG1 were upregulated later in BMPC (Fig. 4F–G). Only a small subset of FLs manifested higher levels of NOTCH ligands. In contrast ADAM 10 and ADAM 17 are expressed in the cell lines, primary mature B-cells and FLs, especially ADAM17 (Fig. 4D, 4H). Hence in the *in vivo* setting NOTCH ligand delivery to lymphoma cells likely comes mostly from the lymph node microenvironment, where NOTCH ligands are known to be expressed (32), whereupon FLs or mature B-cells are then competent to cleave NOTCH2. Indeed we observed that co-culture of FL cells with a stromal cell line engineered to express DLL1 but not the same cell line without DLL1 reproducibly induced apoptosis, consistent with NOTCH2 signaling being deleterious to these cells (Fig. 4I).

BCL6 maintains the survival of FL cells in a *NOTCH2*-dependent manner

To determine whether BCL6 repression of *NOTCH2* was important to its actions in FL cells we first wished to establish whether FL cells are biologically dependent on BCL6. We therefore exposed DoHH2, Sc-1, and WSU-DLCL2 FL-derived cell lines to increasing concentrations of RI-BPI and measured cell viability using a fluorometric resazurin reduction method. DoHH2 and Sc-1 cells displayed a GI_{50} of 11.7 μM and 15.2 μM respectively, which is comparable to the GI_{50} of BCL6-dependent DLBCL cells (7), whereas WSU-DLCL2 cells were more resistant (Fig. 5A). Similar to the case of DLBCL(7,9), not all FL cells were responsive to RI-BPI, but the ones that were sensitive underwent apoptosis, as shown in caspase 3/7 cleavage assays and annexin V/7AAD flow cytometry (Fig. 5B and Supplementary Fig. S6A). To determine whether *NOTCH2* repression contributes to the effect of BCL6 in maintaining survival of FL cells we attempted to rescue our panel of BCL6-dependent FL and GCB-DLBCL lymphoma cell lines (DoHH2, Sc-1, SU-DHL-4 and OCI-Ly1) from the effects of BCL6 depletion by preventing *NOTCH2* upregulation using an siRNA approach. We verified knockdown of both transcripts (BCL6 and NOTCH2) in each cell line, using two independent siRNA for both *BCL6* and *NOTCH2* (Supplementary Fig. S6B). BCL6 knockdown resulted in a ~30–60% loss of viability in all four cell lines at 48h whereas *NOTCH2* siRNA alone did not affect cell viability (Fig. 5C and Supplementary Fig. S6C). Notably, concordant knockdown of NOTCH2 prevented its upregulation in response to BCL6 siRNA and significantly rescued all of four cell lines from BCL6 siRNA induced loss of viability. We used two independent siRNA sequences for BCL6 and NOTCH2. The rescue of siBCL6-1 sequence by both siNOTCH2 RNA sequences is shown in Figure 5C and the rescue of siBCL6-2 in Supplementary Figure S6C. In contrast the viability of the BCL6 independent t(14;18) lymphoma cell line OCI-Ly8 (8) was not affected by BCL6 or NOTCH2 siRNA, even though they manifested a similar degree of knockdown (Supplementary Fig. S6D–E). NOTCH2 siRNA also at least partially rescued FL cells from

loss of viability induced by the BCL6 inhibitor RI-BPI (Fig. 5D and data not shown). In a reciprocal experiment, to determine whether induction of Notch2 was sufficient to suppress the growth of FL cells downstream of BCL6 inhibition, we transduced DoHH2 and Sc-1 cells with a retrovirus expressing ICN2 and GFP, or GFP alone. We measured the relative depletion of GFP positive cells from the total population of cells by flow cytometry over the course of ten days. *NOTCH2* expression was clearly growth suppressive and sufficient to inhibit FL cells since 95% of ICN2-GFP DoHH2 cells were depleted by ten days, as were 75% of ICN2-GFP Sc-1 cells (Supplementary Fig. S6F). Finally, to confirm the importance of NOTCH2 pathway suppression by BCL6 in FL cells, we exposed lymphoma cells to the NOTCH2 antagonist antibody NRR2, after confirming its specificity of action *in vivo* against Notch2 but not Notch1, consistent with previous reports (Supplementary Figure 7) (33,34). NRR2, but not control antibody could also rescue DoHH2 and SU-DHL-4 cells from cell death induced by RI-BPI to variable degrees (Fig. 5E). Repression of NOTCH2 is thus a critical downstream mechanism of action of BCL6, required for its ability to maintain the survival of follicular lymphoma cells.

BCL6 inhibitors suppress FL xenografts *in vivo* and primary human FLs *ex vivo*

FL cell lines may not necessarily accurately represent the biology of primary indolent FL in human patients at the time of diagnosis. We obtained a set of seventeen diagnostic primary human FL specimens from patients with non-transformed disease, made single cell suspensions, exposed them to RI-BPI or vehicle *ex vivo* for 48 hours and then assessed for viability. Immunohistochemistry analysis indicated that 10 patients were clearly BCL6 positive and 7 were borderline positive to negative for BCL6 (data not shown). All 17 samples were exposed to 10 μM RI-BPI or vehicle. While the BCL6 negative/low FLs were resistant to BCL6 inhibitors, 9 out of 10 of the BCL6 positive FLs responded with a 20 to 70% loss of viability (Fig. 6A). Consistent with the actions of BCL6 in normal GC B-cells and FL cell lines, we observed that in primary human FLs, RI-BPI induced derepression of NOTCH2, as well as induction of the NOTCH2 targets HES1 and HES6 (Fig. 6B). Moreover, we also observed re-expression of *ATF5, APOL6, CCR6*, and *HOXA13*, all of which are direct BCL6 targets inversely correlated with BCL6 expression in FL patients (Fig. 1B and Supplementary Table S3), and of *STAT3*, a positive control BCL6 target, but not of *HPRT*, which is a negative control (Supplementary Fig. S8A).

To determine whether RI-BPI could also suppress FL tumors *in situ* in animals, we xenotransplanted the DoHH2 and Sc-1 cell lines into SCID mice. Once palpable tumors formed, pairs of DoHH2 or Sc-1 tumor bearing mice were randomized to receive either RI-BPI 25 mg/kg/day intraperitoneally or vehicle control (5 mice per treatment condition). Both animals of each pair were sacrificed when one of them reached maximal permitted tumor burden. In all cases the RI-BPI treated tumors were considerably smaller than controls both for the more sensitive DoHH2 (Fisher exact test $p=0.03$) and the less sensitive Sc-1 cell line (Fisher exact test $p=0.04$, Fig. 6C). Immunohistochemical analysis of these tumors showed an increase in apoptosis in the RI-BPI treated tumors by TUNEL assays from 7% to 12% in DoHH2 ($p<0.001$, Fisher exact test), and from 10 to 18% ($p<0.001$, Fisher exact test) in Sc-1 tumors respectively. Analysis of these same tumors by Caspase 3 yielded similar results, from 6% to 22% in DoHH2 ($p< 0.0001$, Fisher exact test), and from 11 to 21% ($p<$

0.0001, Fisher exact test) in Sc-1 (Fig. 6D and Supplementary Fig. S8B–D). Examination of mRNA extracted from tumor xenografts revealed upregulation of *NOTCH2, MAML1, MAML2* and *HES1* (p=0.0086, p=0.0011, p=0.0929, and p=0.0079 respectively, Mann-Whitney test) in RI-BPI treated mice vs. vehicle (Fig. 6E). BCL6 is thus a *bona fide* therapeutic target in FL at least in part through its repression of NOTCH2, which we show is a growth suppressor in FL.

Discussion

The role of *BCL6* in FL has not been previously explored, in part because of considerations such as i) the indolent phenotype of FL distinct from the more aggressive DLBCLs typically associated with *BCL6*, ii) the frequent t(14:18) translocation focused attention on *BCL2*, and iii) *BCL6* is not often translocated in FL (5). However, our previous work indicated that DLBCL cells are dependent on BCL6 regardless of whether its locus is affected by mutations (7,8). Therefore analysis of BCL6 in this disease seemed warranted (35,36). Analysis of the BCL6 cistrome in primary FL specimens suggested new mechanisms of action for BCL6 not previously gleaned from studies in DLBCL.

In particular we focused on BCL6 repression of NOTCH2, a growth suppressor of pre-B leukemia cells and Hodgkin lymphoma cells (37). BCL6 was bound to NOTCH target genes in FL and *NOTCH2* levels were inversely correlated with BCL6 in FL. We find that BCL6 is a direct repressor of *NOTCH2, MAML1, MAML2* expression, and that BCL6 inhibition induces NOTCH2 transcriptional activity in reporter assays and endogenous NOTCH2 target genes in FL cells. BCL6 was also shown to antagonize NOTCH signaling in the context of *Xenopus* embryonic development (38). In that setting BCL6 binding and repression of certain Notch target genes as well as its direct interference in the Notch1-MAML1 interaction was essential in the determination of axis symmetry during development (38). In mammals, BCL6 does not play a role in axis symmetry since BCL6 null mice do not show this developmental defect, and antagonism with Notch signaling is more linked to NOTCH2, at least in B-cells. More recently, it was also reported that BCL6 may control neurogenesis through Sirt1-dependent repression of selective Notch targets (39). BCL6 prevented transcriptional activation of *Hes5* promoter, by excluding *Maml1* and instead recruiting *Sirt1* to Notch transcriptional complex to downregulate its expression but without impairing Notch signaling during the transition form neuronal progenitor stem cells to differentiated neurons (39). This additional protein interference mechanism may be relevant to B-cells as well and could be the subject of further investigation into BCL6 and Notch crosstalk.

During B-cell development, induction of Notch2 activity by its ligand DLL1 in the murine splenic vasculature direct B-cells towards marginal zone differentiation and away from the pool of naïve follicular B-cells from which germinal centers form (40). We confirm that *NOTCH2, MAML1* and several key Notch targets are downregulated in GC B-cells in comparison to their precursor naïve B-cells. Indeed we show that Notch2 must be silenced for the development of fully established GCs, and that it is the transcription factor BCL6, which is a master regulator of GC formation that mediates this downregulation. Induction of BCL6 through IL21 and IL4 in human and murine naïve B-cells (23,24) thus resulted in downregulation of *NOTCH2, MAML2* and *RBP-Jk*, suggesting additional mechanisms

through which NOTCH2 activity is controlled in divergent cell fates in secondary lymphoid tissues. BCL6 repression of *NOTCH2* in FL is therefore derived from a normal function of BCL6 in GC B-cells. It is notable that studies in human GC B-cells cultured in the presence of the follicular dendritic HK cell line showed that Jg1-mediated Notch signaling contributes to the survival mediated by follicular dendritic cells (32). In murine B-cells Notch signaling through DLL1 was shown to enhance formation of IgG1 class switched plasma cells (41). However, in experiments with B-cells in their physiological context we show that induction of ICN2 profoundly suppresses GC formation. Along with NOTCH2, BCL6 represses other growth and survival genes in GC B-cells including BCL2 and MYC (10). Collectively, the data suggest a scenario whereby BCL6 may attenuate Notch2 signaling in GC centroblasts in GC dark zone, but later, as BCL6 levels are downregulated and B-cells undergo class switch recombination and interact with follicular dendritic cells of the GC as they transition to memory or plasma cells, Notch pathway may cooperate with other survival signals to maintain the survival and proliferation of post-GC B-cells. Along these lines, Lee et. al. reported five cases of activating NOTCH2 mutations in non-GCB DLBCLs (42), which originate from post-GC B-cells. These findings underline the importance of cell context in determining whether certain genes function as oncogenes or tumor suppressors.

It should be noted that a recent study reported five *NOTCH1* and two *NOTCH2* gain-of-function mutations in FL, accounting for a total of 6.3% among 112 FL patients. However NOTCH-mutated FL cases more frequently included a DLBCL histological component than the WT cases (43). Hence these mutations could occur in very specific subsets of patients who may be borderline DLBCL. Along these lines, Dr. Paulli's work points to a bias towards DLBCL patients positive for hepatitis C virus that carry NOTCH2 mutations (20%) versus the patients negative for the virus (44). They could also be linked to FLs with features of late GC lymphomas. Cell-type context is clearly important since even though NOTCH activating mutations are known to drive T-cell leukemias, NOTCH is by contrast a tumor suppressor in myeloid leukemia (45). Suppression of Notch is evidently a critical function of BCL6 in FLs, since NOTCH2 siRNA or antagonist could rescue cell death induced by BCL6 blockade, and NOTCH2 expression killed FL cells. NOTCH2 is thus a growth suppressor of follicular lymphomas, and BCL6 mediates FL pathogenesis in part through suppression of this pathway.

Finally, we show that BCL6 is a *bona fide* therapeutic target in FL, and not just a passenger marker. This was confirmed using two different loss-of-function strategies (siRNA and RI-BPI) and was relevant not only to cell lines but also to primary human BCL6-positive FLs. BCL6 inhibitors also induced *NOTCH2* and suppressed the growth of FL xenografts, suggesting that cell autonomous inhibition of an FL survival pathway is able to suppress FL tumor growth *in vivo*. This is an example of "non-oncogene" dependence, in that even though the BCL6 locus is not usually mutated in FL, cells that express it are biologically dependent on its continued presence to maintain their survival. Since RI-BPI blocks only the BTB domain lateral groove and does not affect other BCL6 functions, FL survival is clearly dependent on BCL6 recruitment of corepressors to the BCL6 BTB domain (7). The presented data suggest that BCL6 targeted therapy could be a useful approach for treatment of FLs. Importantly, since RI-BPI only affects certain BCL6 functions (46) it does not induce toxicity or inflammation in animals even when administered long-term and so is

suitable as a therapeutic agent for diseases that might require chronic dosing (7). Likewise animals engineered to express a BCL6 mutant that mimics the loss of function induced by RI-BPI live normal healthy lives (47). The data expand the spectrum of patients who are candidates for RI-BPI or other BCL6 inhibitor clinical trials and offer a potential approach for more effectively eradicating these incurable tumors.

Materials and Methods

Gene expression microarray data and RNA-seq

Publically available gene expression microarray data were obtained from 191 primary FLs (9). Data processing and normalization were performed as previously described (9). For the examination of available gene expression profiles obtained from five independent sets of NB and GC B-cells, data publicly available was obtained from GC B-cell array accession number: GSE2350 (22). BCL6 ChIP-on-chip data has been submitted to GEO GSE29165.

Cell lines and reagents

DoHH2, Sc-1, WSU-DLCL2 and SU-DHL-4 cell lines were obtained from the DSMZ German collection of microorganisms and cell cultures. They were grown in RPMI1640 medium (CellGro, Manassas, VA) supplemented with 10% FBS, 1% Penicillin/Streptomycin, 2 mM L-Glutamine and 10 mM HEPES (all from Gibco, Carlsbad, CA). OCI-Ly1 and OCI-Ly8 cell lines were obtained from OCI were grown in Iscove's medium (CellGro, Manassas, VA) supplemented with 10% FBS, 1% Penicillin/Streptomycin as above. Stable cultures for DoHH2 and Sc-1 cell lines were established by retroviral infection of pMigR1-GFP control and pMigR1-ICN2-GFP (the intracellular domain of Notch2 protein that is fused to GFP). OP9 cell line was grown in DMEM medium (Cell Gro, Manassas, VA). Supplemented with 20% FBS, 1% Penicillin/Streptomycin, 2 mM L-Glutamine and 10 mM HEPES 55 μM β-mercaptoethanol and 50 μg/ml Gentamicin (Gibco, Carlsbad, CA).

We performed DNA genotyping to identify and authenticate all the cell lines before use, being December 2016 last time they were authenticated. DNA extraction, short repeat profiling and comparison with known cell line profiles from ATCC were performed by BioSynthesis Inc.

The Retro-inverted BCL6-peptide inhibitor (RI-BPI) corresponds to sequence S6.2 as previously published (7). Control and RI-BPI peptides were synthesized by Biosynthesis Inc. (Lewisville, TX).

Primary B-cell populations' isolation, culture conditions and cytokine treatments

Tonsillar tissue was obtained as discarded material from routine tonsillectomies at the Montefiore Children's Hospital and WCMC (with approval of Institutional Review Boards of Albert Einstein College of Medicine, Montefiore Hospital and Weill Cornell Medical College and in accordance with the Helsinki protocols). Briefly, Tonsillar mononuclear cells were separated by density centrifugation with Fico/Lite LymphoH (Atlanta Biologicals, Norcross, GA). Samples were divided in two and the mononuclear cells rophatPro Separator system as follows: Naïve B cells were stained sequentially with anti-IgD-FITC followed by

FITC-microbeads and performed a positive selection. GC B-cell isolation was done sequentially with anti-CD77, followed by anti-MARM, and a rat anti-mouse IgG1 microbeads followed by a positive selection. The purity of the isolated B cell populations was determined by flow cytometry LSRII system. Naïve B cells are $IgD^{+}CD38^{lo}$ and GC B-cells are $IgD^{-}CD77^{+}CD38^{hi}$ (see Fig. S3 for purity of samples). The FlowJo software from Treestar, Inc. (Ashland, OR) was used for the flow cytometry analysis. Following purification, the samples were processed for mRNA and protein extraction. Naïve B cells were co-cultured with a stromal layer of OP9. Co-cultures were grown in RPMI with 20% FBS, 1%PS, 2mM L-Glutamine and 10 mMHepes. Cytokine treatment was done using 30 ng/ml of IL4 and 30 ng/ml of IL21 or vehicle for up to 4 days. Cell viability was assessed every day by Trypan blue dye-exclusion and cytokines were added to media every other day. Alternatively, resting B lymphocytes from BL57/6 mice spleens were isolated. $B220^{+}$ splenocytes were obtained by negative selection with anti-CD43 and anti-Mac-1/CD11b monoclonal antibodies coupled to magnetic microbeads. Additional information on methods section of Supplementary Figures.

ICN2 knock in mice and NP and SRBC immunization

Experiments were performed in accordance to the guidelines of the New York University Institutional Animal Care and Use Committee. ROSA26-ICN2-IRES-YFP knock-in mice were generated by insertion of a loxP flanked splice acceptor NEO-ATG cassette with two polyA sites followed by the ICN2-IRES-YFP cassette into the ROSA26 locus, allowing the ROSA26 promoter to drive the expression of the NEO-ATG cassette. In order to express the transgene (ICN2-IRES-YFP) these mice were crossed with Tamoxifen inducible ROSA26-$CreER^{T2}$ mice expressing $CreER^{T2}$ from the ubiquitously expressed ROSA26 promoter or with the Cγ**C**re. For GC studies, serum of pre-immunized mice (ROSA 26 WT and ROSA26-ICN2-IRES-YFP knock in) was collected one day prior the start of the experiment (day −1). The next day, mice were injected intraperitoneally with 100 μl of ^{4}Hydroxy-^{3}nitrophenylacetyl hapten-chicken gamma globulin (NP_{65}-GCC) in alum (day 0). For $CreER^{T2}$ induction, Tamoxifen was solubilized in corn oil at a concentration of 20mg/mL and one day after NP immunization, a single intraperitoneal injection of 0.2mg/g body weight was administered. Alternatively, mice were immunized intraperitoneally with 500 μl 2% sheep red blood cells (SRBC) in PBS. Serum was collected at day 7 and day 14. Mice were sacrificed and spleens were harvested for IHC and Flow-cytometry analysis. Schematic representation of experiment in Figure S4A. Genotyping primers are listed in Supplementary Table S5. Additional information on methods section of Supplementary Figures.

Flow-cytometry and Immunohistochemistry of GC

$B220^{+}$ splenocytes from WT and ICN2 mice were obtained as described above. For GC B cell population we gated on $B220^{+}$ and GL7 eFluor674 and CD95(Fas) PECy7. For plasma cell population ($CD38^{+}$ $CD138^{+}$) we used CD38 APC and CD138 PE. ICN2 expression was assessed by $B220^{+}$ YFP^{+}. Immunohistochemistry of spleens was performed on formalin-fixed paraffin-embedded sections with the following primary antibodies: PNA, BCL6 (N3) and CD45R/B220. BCL6 shows a purple pattern, while B220 staining is pale brown. To

count the GC we used CellSens Software (Olympus America Inc.). Additional information on methods section of Supplementary Figures.

Primary lymphoma samples

De-identified primary FL specimen tissues were obtained in accordance with the guidelines and approval of the Institutional Review Board of the Weill Cornell Medical College and in accordance with the Helsinki protocols. We selected the specimens based on estimated tumor content >80% by our collaborating pathologist Dr. Wayne Tam. Single-cell suspensions from lymph node biopsies were obtained by physical disruption of tissues (using scalpels and cell strainers), followed by cell density gradient separation (Fico/Lite LymphoH; Atlanta Biologicals, Norcross, GA). Cell number and viability were determined by trypan blue dye exclusion, and cells were cultivated in medium containing 80% RPMI and 20% human serum supplemented with antibiotics, L-glutamine 4 mM and HEPES 10 mM. Cells were exposed in duplicates to control and RI-BPI at indicated concentrations for 48 h. Viability was determined as detailed above. The BCL6 protein status was determined in paraffin-embedded samples by immunohistochemistry using anti-BCL6 (Dako North America, Carpinteria, CA).

Mice xenotransplant studies

All animal procedures followed NIH protocols and were approved by the Animal Institute Committee of the Weill Cornell Medical College. Six to eight-week old male SCID mice were purchased from the National Cancer Institute (NCI) and housed in a clean environment. Mice were subcutaneously injected in the left flank with low-passage 10^7 human lymphoma cells (DoHH2 and Sc-1). Tumor volume was monitored every other day using electronic digital calipers in two dimensions. Tumor volume was calculated using the formula: Tumor Volume (mm^3) = (smallest diameter^2 × largest diameter)/2. When tumors reached a palpable size (approximately 75 to 100 mm^3 after 21 days post-injection), the mice were randomized to two different treatment arms. RI-BPI was stored lyophilized at −20C until reconstituted with sterile pure water immediately before used. RI-BPI was administered by intra-peritoneal injection. Mice were weighed twice a week. All mice were euthanized by cervical dislocation under anesthesia when at least 2/10 tumors reached 20 mm in any dimension (equivalent to 1 gram), which was generally on day 9 or 10 of the treatment schedule. At the moment of euthanasia the tumors and other tissues were harvested and weighed.

Transfections, anti-NRR2 and RI-BPI treatment of lymphoma cell lines

For siRNA knockdown experiments BCL6 specific siRNAs (Cat# HSS100966) and control non-targeting siRNA (Cat# 1299003) were purchased from Invitrogen (Invitrogen, Carlsbad, CA). siRNA sequences for NOTCH2 (Cat# J-012235) were purchased from Dharmacon-ThermoScientific (Rockfold, IL). 20pmol siRNA was suspended in 20 μl of Solution SF and introduced into 3×10^6 cells using the Amaxa 96-well nucleofector (Lonza, Walkersville, MD). For Western blot experiments, rabbit antibody raised against BCL6-N3 (sc-858) and anti-Actin-HRP conjugated (sc-1615) were purchased from Santa Cruz Biotechnology (Santa Cruz, CA), rabbit antibody raised against ICN2 (ab72803) that recognizes the cleaved intracellular fragment of Notch2 was purchased from Abcam (Cambridge, MA). For

experiments using cell lines treated with RI-BPI, 10 to 20 μM final concentration of the drug were used for 24 and 48 hours. Doses were selected based on the relative GI50s for each cell line. For DoHH2 and Sc-1 anti-NRR2 experiments, 2×10^6 cells were treated with 2 μg/ml of anti-NRR2 from Genentech, Inc. (South San Francisco, CA) or a negative control, anti-IgG1 from Southern Biotech (Birmingham, AL). 24 h post-treatment cells were re-plated to 96-well plates and RI-BPI was added. Cell viability was measured 24 or 48 hours after RI-BPI treatment as detailed in cell viability assay section. Experiments were performed in triplicates and the figures represent the average of three experiments +/− SEM.

Cell viability assay and growth inhibition determination

Cell viability on lymphoma cell lines was determined using a fluorometric resazurin reduction method (CellTiter-Blue, Promega, Madison, WI) and relative fluorescence ($560_{exitation}/590_{emission}$) detected with a Synergy4 Microplate Reader (BioTek Instruments, Winooski, VT). The number of viable cells was calculated by extrapolating from the standard curve. Fluorescence was measured for three replicates per treatment condition and cell viability in drug-treated cells normalized to their respective controls. Experiments were performed in triplicates. The figures represent the average of three experiments and the standard error of the mean (SEM). To determine growth inhibition of lymphoma cell lines exposed to different doses of RI-BPI, cells were plated at concentrations sufficient to keep untreated cells in exponential growth over the 48h drug exposure time. Cell viability was measured as described above. Trypan blue dye-exclusion was used as a secondary method to confirm the results. Fluorescence was determined for 6 replicates per treatment condition and cell viability in drug-treated cells was normalized to their respective controls. Unless stated otherwise, the experiments were carried out in biological triplicates. The CompuSyn software package (Biosoft, Cambridge, UK) was used to plot dose-effect curves and determine the drug concentration that inhibits the growth of cell lines by 50% compared to control (GI_{50}). The linear correlation coefficient was higher than 0.90 for each curve in the median-effect plot.

Additional Experimental Procedures including quantitative RT-PCR, plasmids and reporter assays, ChIP and ChIP-on-ChIP assay, Bioinformatics analysis of Gene Expression data, primary cultures, flow cytometry and mice studies can be found on Supplemental Experimental Procedures.

Supplementary Material

Refer to Web version on PubMed Central for supplementary material.

Acknowledgments

We thank the Weill Cornell Epigenomics Core Facility for support with ChIP-on-chip assays. We thank Dr. Artavanis-Tsakonas for sharing the ROSA26-NOTCH2IC animals.

Financial Support. This research was funded by a follicular lymphoma research grant from the Lymphoma Research Foundation to AM. AM is also supported by NCIR01CA104348, NCIR01CA143032, and the Chemotherapy Foundation. EV has been the recipient of an IDIBAPS Postdoctoral Fellowship-BIOTRACK, supported by the European Community's Seventh Framework Programme (EC FP7/2007–2013) under the grant agreement number 229673. I.A. is supported by the NIH (RO1CA216421, RO1CA169784, RO1CA202025, R01CA133379, R01CA149655) and the NYSTEM program of the New York State Health Department. C.L. is

supported by a Leukemia and Lymphoma Society Career development award and a French government ATIP-Avenir grant. WC is supported from the National Basic Research Programme (Grant No. 2016YFC0900303); the National Natural Science Foundation of China (Grant No. 81422035, 91519307, 81672541 and CAS (Grant No. QYZDB-SSW-SMC039 and KJZD-EW-L14).

References

1. Tan D, Horning SJ. Follicular lymphoma: clinical features and treatment. Hematol Oncol Clin North Am. 2008; 22(5):863–82. viii. doi S0889-8588(08)00109-3 [pii]10.1016/j.hoc.2008.07.013. [PubMed: 18954741]
2. Piccaluga PP, Sapienza MR, Agostinelli C, Sagramoso C, Mannu C, Sabattini E, et al. Biology and treatment of follicular lymphoma. Expert Rev Hematol. 2009; 2(5):533–47. DOI: 10.1586/ehm.09.49 [PubMed: 21083019]
3. Egle A, Harris AW, Bath ML, O'Reilly L, Cory S. VavP-Bcl2 transgenic mice develop follicular lymphoma preceded by germinal center hyperplasia. Blood. 2004; 103(6):2276–83. 2003-07-2469 [pii]. DOI: 10.1182/blood-2003-07-2469 [PubMed: 14630790]
4. Skinnider BF, Horsman DE, Dupuis B, Gascoyne RD. Bcl-6 and Bcl-2 protein expression in diffuse large B-cell lymphoma and follicular lymphoma: correlation with 3q27 and 18q21 chromosomal abnormalities. Hum Pathol. 1999; 30(7):803–8. [PubMed: 10414499]
5. Swerdlow, SH., Campo, E., Harris, NL., Jaffe, ES., Pileri, SA., Thiele, J., et al. WHO Classification of Tumours of Haematopoietic and Lymphoid Tissues. Fourth. Geneva, Switzerland: WHO Press; 2008.
6. Hatzi K, Melnick A. Breaking bad in the germinal center: how deregulation of BCL6 contributes to lymphomagenesis. Trends in molecular medicine. 2014; 20(6):343–52. DOI: 10.1016/j.molmed.2014.03.001 [PubMed: 24698494]
7. Cerchietti LC, Yang SN, Shaknovich R, Hatzi K, Polo JM, Chadburn A, et al. A peptomimetic inhibitor of BCL6 with potent antilymphoma effects in vitro and in vivo. Blood. 2009; 113(15):3397–405. doi blood-2008-07-168773 [pii] 10.1182/blood-2008-07-168773. [PubMed: 18927431]
8. Polo JM, Dell'Oso T, Ranuncolo SM, Cerchietti L, Beck D, Da Silva GF, et al. Specific peptide interference reveals BCL6 transcriptional and oncogenic mechanisms in B-cell lymphoma cells. Nature medicine. 2004; 10(12):1329–35. doi nm1134 [pii] 10.1038/nm1134.
9. Polo JM, Juszczynski P, Monti S, Cerchietti L, Ye K, Greally JM, et al. Transcriptional signature with differential expression of BCL6 target genes accurately identifies BCL6-dependent diffuse large B cell lymphomas. Proc Natl Acad Sci U S A. 2007; 104(9):3207–12. doi 0611399104 [pii]10.1073/pnas.0611399104. [PubMed: 17360630]
10. Ci W, Polo JM, Cerchietti L, Shaknovich R, Wang L, Yang SN, et al. The BCL6 transcriptional program features repression of multiple oncogenes in primary B cells and is deregulated in DLBCL. Blood. 2009; 113(22):5536–48. doi blood-2008-12-193037 [pii]10.1182/blood-2008-12-193037. [PubMed: 19307668]
11. Elemento O, Slonim N, Tavazoie S. A universal framework for regulatory element discovery across all genomes and data types. Mol Cell. 2007; 28(2):337–50. doi S1097-2765(07)00666-1 [pii]10.1016/j.molcel.2007.09.027. [PubMed: 17964271]
12. Shaffer AL, Yu X, He Y, Boldrick J, Chan EP, Staudt LM. BCL-6 represses genes that function in lymphocyte differentiation, inflammation, and cell cycle control. Immunity. 2000; 13(2):199–212. [pii]. [PubMed: 10981963]
13. Alizadeh AA, Eisen MB, Davis RE, Ma C, Lossos IS, Rosenwald A, et al. Distinct types of diffuse large B-cell lymphoma identified by gene expression profiling. Nature. 2000; 403(6769):503–11. DOI: 10.1038/35000501 [PubMed: 10676951]
14. Whitfield ML, Sherlock G, Saldanha AJ, Murray JI, Ball CA, Alexander KE, et al. Identification of genes periodically expressed in the human cell cycle and their expression in tumors. Molecular biology of the cell. 2002; 13(6):1977–2000. DOI: 10.1091/mbc.02-02-0030 [PubMed: 12058064]
15. Palomero T, Lim WK, Odom DT, Sulis ML, Real PJ, Margolin A, et al. NOTCH1 directly regulates c-MYC and activates a feed-forward-loop transcriptional network promoting leukemic cell growth. Proc Natl Acad Sci U S A. 2006; 103(48):18261–6. doi 0606108103 [pii]10.1073/pnas.0606108103. [PubMed: 17114293]

16. Shaffer AL, Lin KI, Kuo TC, Yu X, Hurt EM, Rosenwald A, et al. Blimp-1 orchestrates plasma cell differentiation by extinguishing the mature B cell gene expression program. Immunity. 2002; 17(1):51–62. [PubMed: 12150891]

17. Dave SS, Wright G, Tan B, Rosenwald A, Gascoyne RD, Chan WC, et al. Prediction of survival in follicular lymphoma based on molecular features of tumor-infiltrating immune cells. N Engl J Med. 2004; 351(21):2159–69. doi 351/21/2159 [pii]10.1056/NEJMoa041869. [PubMed: 15548776]

18. Sharma VM, Calvo JA, Draheim KM, Cunningham LA, Hermance N, Beverly L, et al. Notch1 contributes to mouse T-cell leukemia by directly inducing the expression of c-myc. Mol Cell Biol. 2006; 26(21):8022–31. doi MCB.01091-06 [pii]10.1128/MCB.01091-06. [PubMed: 16954387]

19. Weng AP, Millholland JM, Yashiro-Ohtani Y, Arcangeli ML, Lau A, Wai C, et al. c-Myc is an important direct target of Notch1 in T-cell acute lymphoblastic leukemia/lymphoma. Genes Dev. 2006; 20(15):2096–109. doi gad.1450406 [pii]10.1101/gad.1450406. [PubMed: 16847353]

20. Dave SS, Fu K, Wright GW, Lam LT, Kluin P, Boerma EJ, et al. Molecular diagnosis of Burkitt's lymphoma. N Engl J Med. 2006; 354(23):2431–42. DOI: 10.1056/NEJMoa055759 [PubMed: 16760443]

21. Saito T, Chiba S, Ichikawa M, Kunisato A, Asai T, Shimizu K, et al. Notch2 is preferentially expressed in mature B cells and indispensable for marginal zone B lineage development. Immunity. 2003; 18(5):675–85. [pii]. [PubMed: 12753744]

22. Basso K, Margolin AA, Stolovitzky G, Klein U, Dalla-Favera R, Califano A. Reverse engineering of regulatory networks in human B cells. Nat Genet. 2005; 37(4):382–90. doi ng1532 [pii]10.1038/ng1532. [PubMed: 15778709]

23. Linterman MA, Beaton L, Yu D, Ramiscal RR, Srivastava M, Hogan JJ, et al. IL-21 acts directly on B cells to regulate Bcl-6 expression and germinal center responses. The Journal of experimental medicine. 2010; 207(2):353–63. doi jem.20091738 [pii]10.1084/jem.20091738. [PubMed: 20142429]

24. Tsuruoka N, Arima M, Arguni E, Saito T, Kitayama D, Sakamoto A, et al. Bcl6 is required for the IL-4-mediated rescue of the B cells from apoptosis induced by IL-21. Immunol Lett. 2007; 110(2): 145–51. doi S0165-2478(07)00096-X [pii]10.1016/j.imlet.2007.04.009. [PubMed: 17532053]

25. Oh P, Lobry C, Gao J, Tikhonova A, Loizou E, Manent J, et al. In vivo mapping of notch pathway activity in normal and stress hematopoiesis. Cell Stem Cell. 2013; 13(2):190–204. DOI: 10.1016/j.stem.2013.05.015 [PubMed: 23791481]

26. Casola S, Cattoretti G, Uyttersprot N, Koralov SB, Seagal J, Hao Z, et al. Tracking germinal center B cells expressing germ-line immunoglobulin gamma1 transcripts by conditional gene targeting. Proc Natl Acad Sci U S A. 2006; 103(19):7396–401. DOI: 10.1073/pnas.0602353103 [PubMed: 16651521]

27. Hatzi K, Jiang Y, Huang C, Garrett-Bakelman F, Gearhart MD, Giannopoulou EG, et al. A hybrid mechanism of action for BCL6 in B cells defined by formation of functionally distinct complexes at enhancers and promoters. Cell reports. 2013; 4(3):578–88. DOI: 10.1016/j.celrep.2013.06.016 [PubMed: 23911289]

28. Cerchietti LC, Hatzi K, Caldas-Lopes E, Yang SN, Figueroa ME, Morin RD, et al. BCL6 repression of EP300 in human diffuse large B cell lymphoma cells provides a basis for rational combinatorial therapy. The Journal of clinical investigation. 2010; 120(12):4569–82. DOI: 10.1172/JCI42869 [PubMed: 21041953]

29. Cerchietti LC, Polo JM, Da Silva GF, Farinha P, Shaknovich R, Gascoyne RD, et al. Sequential transcription factor targeting for diffuse large B-cell lymphomas. Cancer Res. 2008; 68(9):3361–9. DOI: 10.1158/0008-5472.CAN-07-5817 [PubMed: 18451163]

30. Ortega-Molina A, Boss IW, Canela A, Pan H, Jiang Y, Zhao C, et al. The histone lysine methyltransferase KMT2D sustains a gene expression program that represses B cell lymphoma development. Nature medicine. 2015; 21(10):1199–208. DOI: 10.1038/nm.3943

31. Jiang Y, Ortega-Molina A, Geng H, Ying HY, Hatzi K, Parsa S, et al. CREBBP Inactivation Promotes the Development of HDAC3-Dependent Lymphomas. Cancer Discov. 2017; 7(1):38–53. DOI: 10.1158/2159-8290.CD-16-0975 [PubMed: 27733359]

32. Yoon SO, Zhang X, Berner P, Blom B, Choi YS. Notch ligands expressed by follicular dendritic cells protect germinal center B cells from apoptosis. J Immunol. 2009; 183(1):352–8. doi 183/1/352 [pii] 10.4049/jimmunol.0803183. [PubMed: 19542446]
33. Tran IT, Sandy AR, Carulli AJ, Ebens C, Chung J, Shan GT, et al. Blockade of individual Notch ligands and receptors controls graft-versus-host disease. The Journal of clinical investigation. 2013; 123(4):1590–604. DOI: 10.1172/JCI65477 [PubMed: 23454750]
34. Wu Y, Cain-Hom C, Choy L, Hagenbeek TJ, de Leon GP, Chen Y, et al. Therapeutic antibody targeting of individual Notch receptors. Nature. 2010; 464(7291):1052–7. doi nature08878 [pii]10.1038/nature08878. [PubMed: 20393564]
35. Lee CH, Chawla A, Urbiztondo N, Liao D, Boisvert WA, Evans RM, et al. Transcriptional repression of atherogenic inflammation: modulation by PPARdelta. Science. 2003; 302(5644): 453–7. [pii]. DOI: 10.1126/science.10873441087344 [PubMed: 12970571]
36. Vasanwala FH, Kusam S, Toney LM, Dent AL. Repression of AP-1 function: a mechanism for the regulation of Blimp-1 expression and B lymphocyte differentiation by the B cell lymphoma-6 protooncogene. J Immunol. 2002; 169(4):1922–9. [PubMed: 12165517]
37. Zweidler-McKay PA, He Y, Xu L, Rodriguez CG, Karnell FG, Carpenter AC, et al. Notch signaling is a potent inducer of growth arrest and apoptosis in a wide range of B-cell malignancies. Blood. 2005; 106(12):3898–906. doi 2005-01-0355 [pii]10.1182/blood-2005-01-0355. [PubMed: 16118316]
38. Sakano D, Kato A, Parikh N, McKnight K, Terry D, Stefanovic B, et al. BCL6 canalizes Notch-dependent transcription, excluding Mastermind-like1 from selected target genes during left-right patterning. Dev Cell. 2010; 18(3):450–62. doi S1534-5807(10)00052-3 [pii]10.1016/j.devcel. 2009.12.023. [PubMed: 20230751]
39. Tiberi L, van den Ameele J, Dimidschstein J, Piccirilli J, Gall D, Herpoel A, et al. BCL6 controls neurogenesis through Sirt1-dependent epigenetic repression of selective Notch targets. Nature neuroscience. 2012; 15(12):1627–35. DOI: 10.1038/nn.3264 [PubMed: 23160044]
40. Pillai S, Cariappa A. The follicular versus marginal zone B lymphocyte cell fate decision. Nature reviews Immunology. 2009; 9(11):767–77. doi nri2656 [pii]10.1038/nri2656.
41. Thomas M, Calamito M, Srivastava B, Maillard I, Pear WS, Allman D. Notch activity synergizes with B-cell-receptor and CD40 signaling to enhance B-cell activation. Blood. 2007; 109(8):3342–50. doi blood-2006-09-046698 [pii]10.1182/blood-2006-09-046698. [PubMed: 17179224]
42. Lee SY, Kumano K, Nakazaki K, Sanada M, Matsumoto A, Yamamoto G, et al. Gain-of-function mutations and copy number increases of Notch2 in diffuse large B-cell lymphoma. Cancer Sci. 2009; 100(5):920–6. [PubMed: 19445024]
43. Karube K, Martinez D, Royo C, Navarro A, Pinyol M, Cazorla M, et al. Recurrent mutations of NOTCH genes in follicular lymphoma identify a distinctive subset of tumours. The Journal of pathology. 2014; 234(3):423–30. DOI: 10.1002/path.4428 [PubMed: 25141821]
44. Arcaini L, Rossi D, Lucioni M, Nicola M, Bruscaggin A, Fiaccadori V, et al. The NOTCH pathway is recurrently mutated in diffuse large B cell lymphoma associated with hepatitis C virus infection. Haematologica. 2014; 100(2):246–52. DOI: 10.3324/haematol.2014.116855 [PubMed: 25381127]
45. Klinakis A, Lobry C, Abdel-Wahab O, Oh P, Haeno H, Buonamici S, et al. A novel tumour-suppressor function for the Notch pathway in myeloid leukaemia. Nature. 2011; 473(7346):230–3. doi nature09999 [pii]10.1038/nature09999. [PubMed: 21562564]
46. Parekh S, Polo JM, Shaknovich R, Juszczynski P, Lev P, Ranuncolo SM, et al. BCL6 programs lymphoma cells for survival and differentiation through distinct biochemical mechanisms. Blood. 2007; 110(6):2067–74. doi blood-2007-01-069575 [pii]10.1182/blood-2007-01-069575. [PubMed: 17545502]
47. Huang C, Hatzi K, Melnick A. Lineage-specific functions of BCL6 in immunity and inflammation are mediated through distinct biochemical mechanisms. Nature immunology. 2013; 14(4):380–8. DOI: 10.1038/ni.2543 [PubMed: 23455674]

Significance

We show that human follicular lymphomas are dependent on BCL6, and primary human follicular lymphomas can be killed using specific BCL6 inhibitors. Integrative genomics and functional studies of BCL6 in primary follicular lymphoma cells point towards a novel mechanism whereby BCL6 repression of NOTCH2 drives the survival and growth of FL cells as well as germinal center B-cells, which are the FL cell of origin.

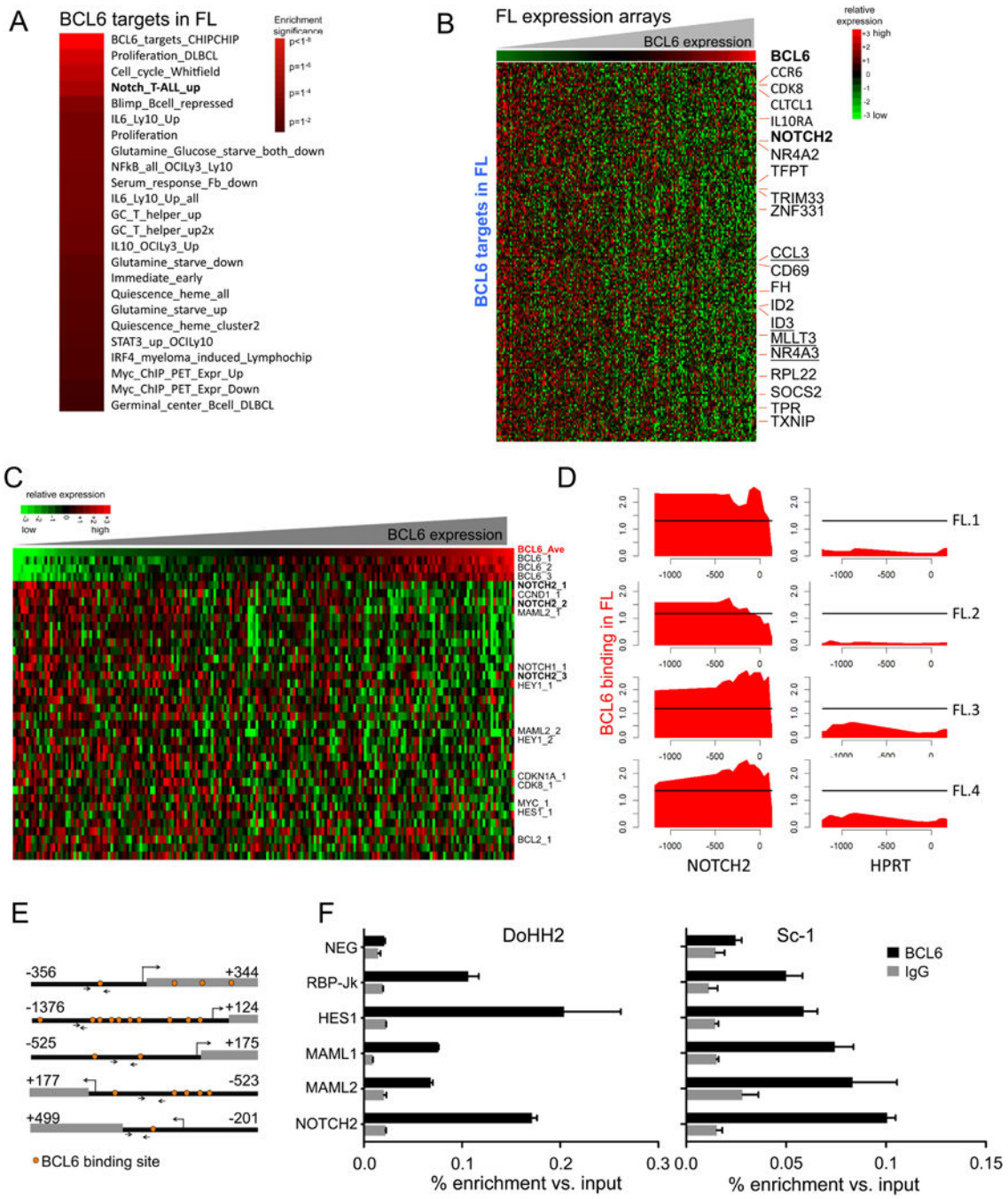

Figure 1. BCL6 displays a specific genomic localization pattern in FL

(**A**) The relative enrichment of specific gene signatures on FL BCL6 target gene sets summarized in a heat map. The statistical significance (BH adjusted p values) is provided in color key. (**B**) A heatmap representation of the relative transcript abundance of BCL6 target genes in FLs that display inverse correlation ($p<0.05$, Spearman correlation) with BCL6 expression, from a publicly available dataset of 191 primary FL expression profiles. The color key indicates the relative expression values. (**C**) Primary FL gene expression profiles were sorted by BCL6 expression from low to high (top row of heatmap), and the relative

expression values of a set of Notch complex and target genes displayed in subsequent rows, indicating their degree of inverse correlation (p values are all $p<0.05$, Spearman correlation) with BCL6. Details are provided in Supplementary Table S4. **(D)** BCL6 binding represented for NOTCH2 and HPRT genes (negative control), in red binding of BCL6 on 4 independent FL patient samples. Y-axis represents read densities normalized to total number of reads. Threshold setting is explained in methods section. Promoter expands to −1000 base pairs (bp) downstream of TSS. (**E**) Cartoon representation of the *RBP-Jk, HES1, MAML1, MAML2* and *NOTCH2* promoter regions indicating BCL6 DNA binding motifs (orange dots) and QChIP amplicon location (arrows). (**F**) QChIP assays were performed in DoHH2 and Sc-1 FL cells using BCL6 antibody (black bars) and IgG (negative control, gray bars) for the genes shown in B and a negative control (NEG). The X-axis represents percent enrichment of BCL6 antibody vs. input DNA. See additional data in Supplementary Figure S1.

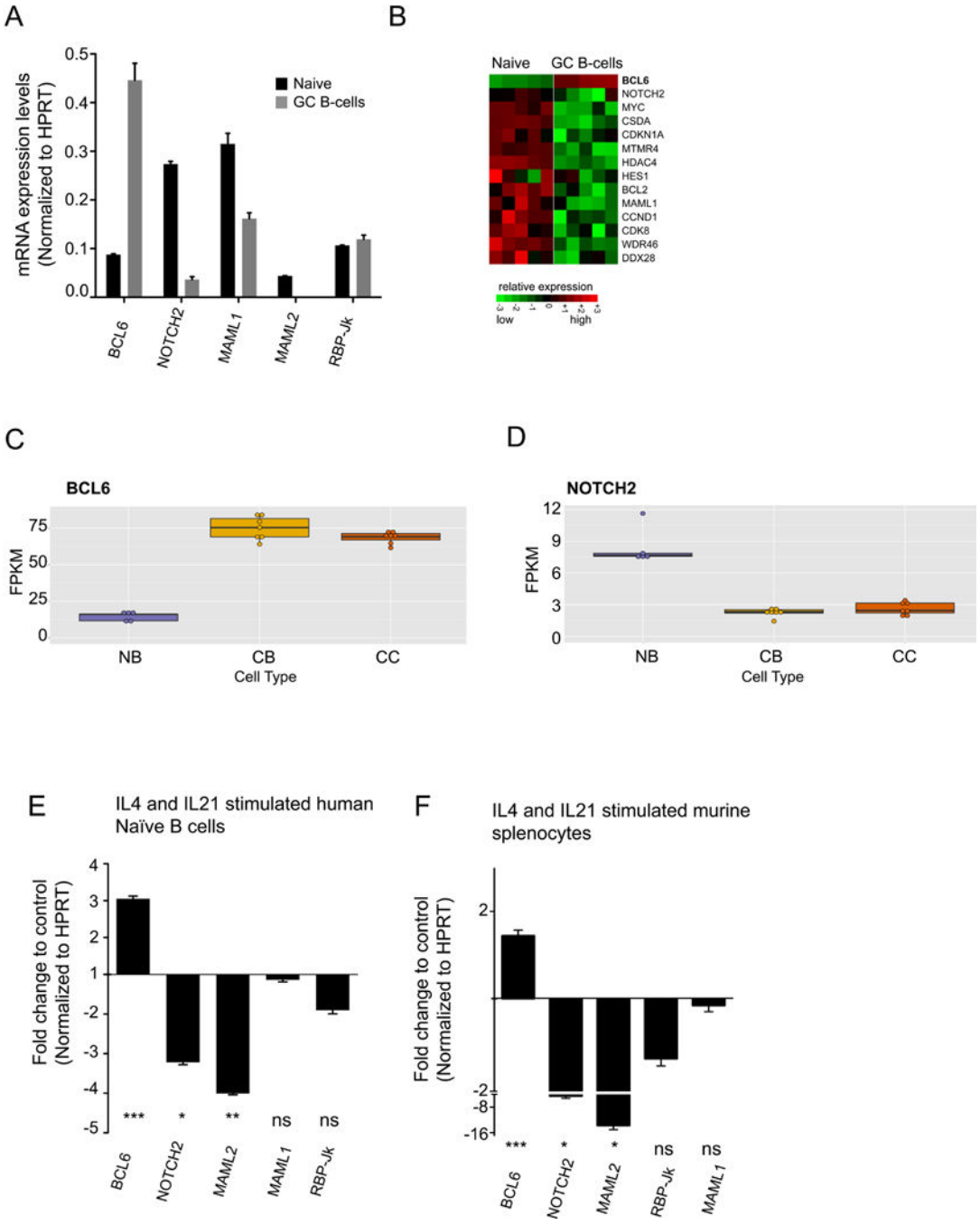

Figure 2. Inverse correlation between BCL6 and NOTCH2 complex genes in primary GC B-cells

(**A**) QPCR was performed in purified human tonsillar naïve B-cells (black) and GC B-cells (gray) to measure the relative transcript abundance of the indicated genes. The Y-axis represents mRNA expression levels normalized to HPRT. (**B**) A heatmap representation of *BCL6, NOTCH2* and Notch complex and target gene expression levels in five human naïve B-cells and five GC B-cell specimens. The color key shows relative expression values. (**C**) Expression values (FPKM) of BCL6 from Naïve B-cells (purple, n=5), Centroblast (yellow, n=7) and Centrocytes (orange, n=7) from independent specimens each. (**D**) Expression

values of NOTCH2 as in panel C. (**E**) Human naïve B cells were cultured with OP9 stromal monolayer and stimulated with IL4 plus IL21 or left untreated. QPCR was performed for the indicated genes. The Y-axis represents the fold change, normalized to HPRT, and relative to vehicle (control) at day 4 when maximum levels of BCL6 were reached. (**F**) Mouse resting $B220^{+}$ cells were isolated and activated with mouse cytokines IL4 and IL21 for 24h. The same rationale as for panel D was followed. For panels A, D and E, the mean of three independent experiments is represented along with the SEM. For panels D and E p values are based on unpaired two-tailed *t* test. See Supplementary Figure S2 for additional information.

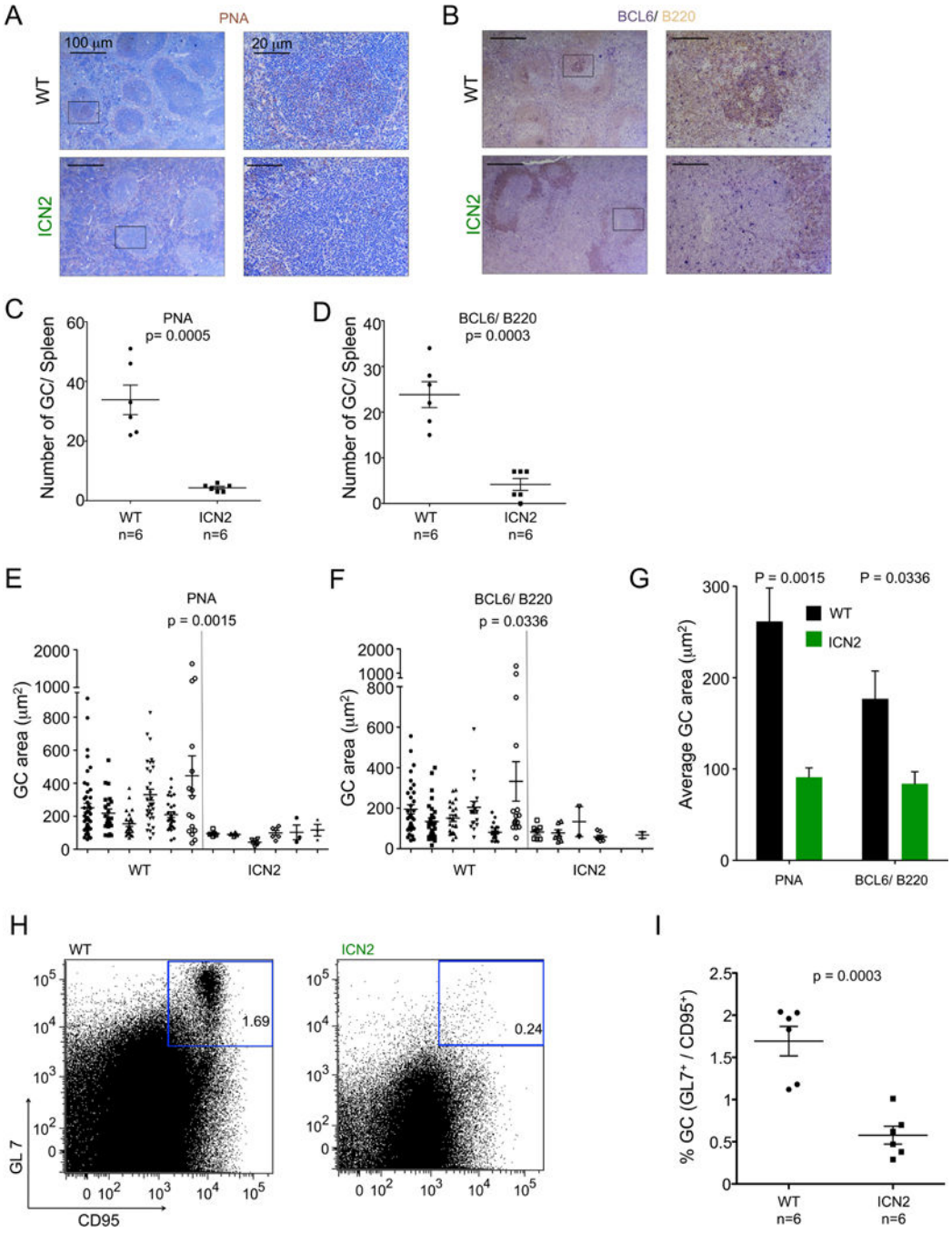

Figure 3. GC reaction is impaired in Notch2 knock-in mice

(**A**) Representative images of spleen sections from WT control and ICN2 knock-in mice stained for GC markers PNA (left) and BCL6$^+$/B220$^+$ (right) 14 days after immunization with NP_{65}-CGG. The black squares on left column (4X) highlight GCs, which are shown at 20X amplification in the right column. Scale bars are 40 μm (10X) and 20 μm (20X). (**B**) The number of GCs per spleen (Y-axis) from immunohistochemistry shown in panel A. PNA$^+$ clusters (left) and BCL6$^+$B220$^+$ clusters (right) are shown. The range bars represent the mean values and SEM and the p values are shown on top. (**C**) The surface area occupied

by GCs in the spleens of immunized and induced ICN2 and control mice is shown for PNA and BCL6/B220 staining respectively, and is represented by their area in μm^2 (Y-axis). The average of the means for each group is shown. Each column corresponds to an individual mouse; each point is an individual GC; p values are shown on top. SEM and p values are shown. (**D**) Average of GC area (μm^2) of WT (black) and ICN2 (green) mice from IHC of paraffin-embedded spleen slides stained with PNA^+ and $BCL6^+/B220^+$ antibodies. The mean values are 261.7 +/−36.48 vs. 91.05 +/−10.22 μm^2 for PNA^+ GC, and 177.1 +/−30.22 vs. 83.93 +/−13.13 μm^2. The statistical significance of this difference is shown based on unpaired two-tailed *t* test (P= 0.0015 and P= 0.0336 respectively). Data shown for immunized WT (n=6) and ICN2 (n=6) mice. (**E**) Flow-cytometry analysis of $B220^+GL7^+CD95^+$ labeled splenic GC B-cell populations. Cells were gated for $B220^+$, GL7 is on the Y-axis and CD95(Fas) is on the X-axis. The percentage of double positive cells corresponds to GC B-cells (black box). (**F**) The percentage of $B220^+$ gated $GL7^+/CD95^+$ GC B-cells among total splenocytes is shown from the spleens of immunized WT (n=6) and ICN2 induced (n=6) mice. In panels B, C and E the statistical values are based on unpaired two-tailed *t* test. (**G**) Average of GC area (μm^2) of WT (black) and ICN2 (green) mice from IHC of paraffin-embedded spleen slides stained with PNA^+ and $BCL6^+/B220^+$ antibodies. The mean values are 262+/−36 vs. 91+/−10 μm^2 for PNA^+ GC, and 177+/−30 vs. 84+/−13 μm^2. Data shown for immunized Cγ Cre-WT (n=5) and Cγ Cre-ICN2 (n=8) mice. The statistical significance of this difference is shown based on unpaired two-tailed *t* test (P= 0.0015 and P= 0.0336 respectively). (**H**) Flow-cytometry analysis of $B220^+GL7^+CD95^+$ labeled splenic GC B-cell populations. Cells were gated for $B220^+$, GL7 is on the Y-axis and CD95(Fas) is on the X-axis. The percentage of double positive cells corresponds to GC B-cells (black box). **(I)** The percentage of $B220^+$ gated $GL7^+/CD95^+$ GC B-cells among total splenocytes is shown from the spleens of immunized WT (n=5) and ICN2 induced (n=8) mice. In the presence of ICN2, the abundance of $B220^+GL7^+CD95^+$ GC B-cells was reduced three-fold as compared to WT animals (1.7% vs. 0.6% mean GC B-cells vs. total splenocytes, p=0.0003 unpaired two-tailed *t* test. See Supplementary Figures S3 and S4 for additional data.

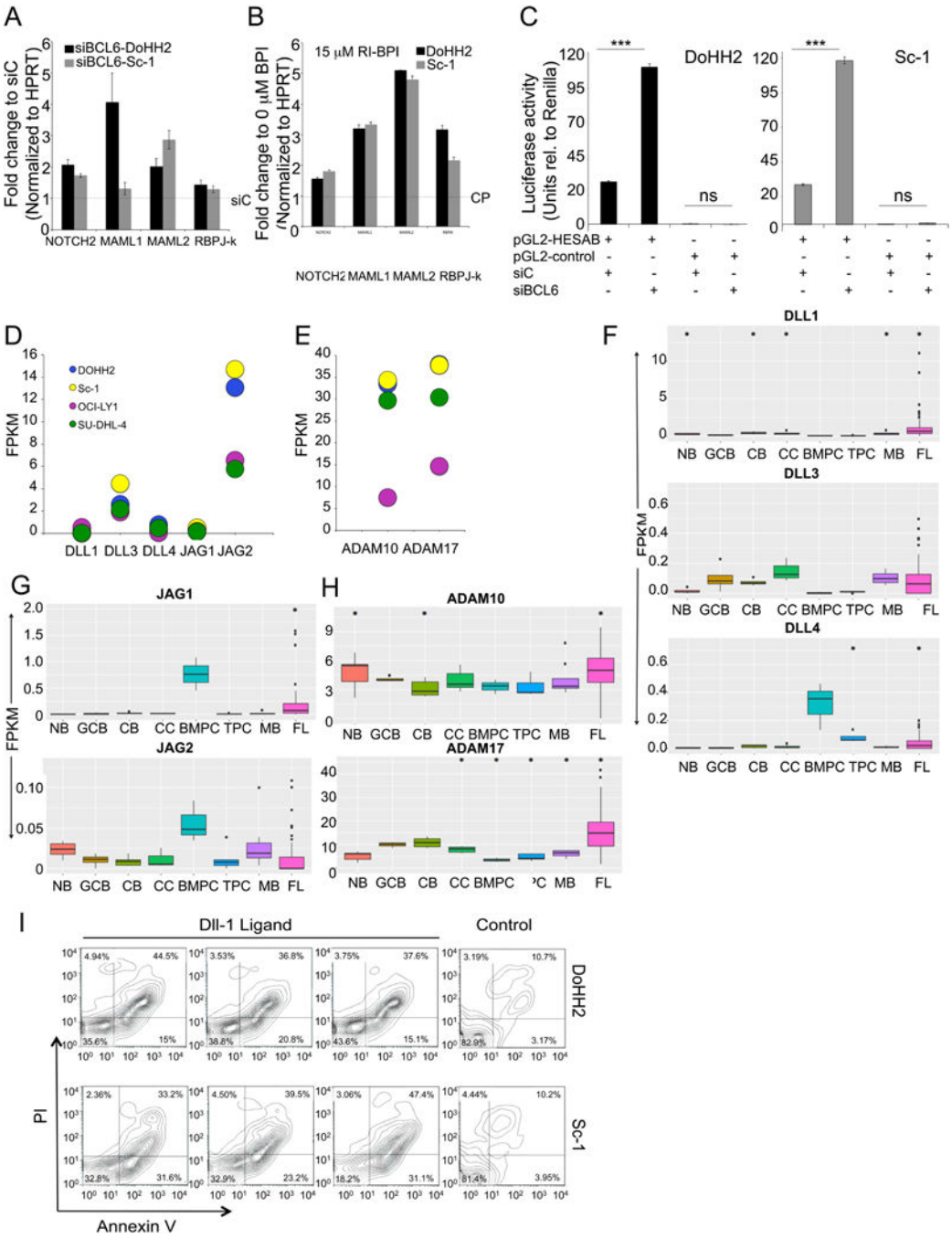

Figure 4. BCL6 represses NOTCH2 complex genes and Notch activity

(**A**) The relative transcript abundance of *NOTCH2, MAML1, MAML2* and *RBPJ-k* was examined by QPCR in DoHH2 (black bars) and Sc-1 (gray bars) 72 h after BCL6 siRNA depletion vs. control siRNA. Values were normalized to HPRT and fold change (Y-axis) is represented over a scrambled siRNA control. (**B**) The relative transcript abundance of *NOTCH2, MAML1, MAML2* and *RBP-Jk* was examined by QPCR in FL cell lines DoHH2 (black bars) and Sc-1 (gray bars) 72 h after RI-BPI treatment (15 μM RI-BPI) in the right panel. Values were normalized to HPRT and fold change (Y-axis) is represented over

Control Peptide (CP). (**C**) Reporter assays performed in DoHH2 (black bars) and Sc-1 (gray bars) cells transfected with pGL2-HESAB (Notch reporter) or pGL2 control vector, and with BCL6 (siBCL6) or control siRNA (siC). The Y-axis shows the luciferase activity relative to renilla (internal control). All panels represent the mean of three independent experiments, each performed in triplicate, and the error bars represent the standard error of the mean (SEM). The statistical values are based on unpaired two-tailed *t* test. (**D**) Expression values (FPKM) of NOTCH ligands DLL1, DLL3, DLL4, JAG1 and JAG2 on DoHH2 (blue), Sc-1 (yellow), OCI-Ly1 (purple), SU-DHL-4 (green). (**E**) As in panel D, expression values (FPKM) of metalloproteases ADAM10 and ADAM17 on the same cell lines. (**F**) Expression values (FPKM) of DLL1 (upper panel), DLL3 (middle panel) and DLL4 (bottom panel) from left to right Naïve B-cells (n=5, NB), Germinal Center B cells (n=4, GCB), Centroblast (n=7, CB), Centrocytes (n=.7, CC), Bone Marrow Plasma Cells (n=3, BMPC), Tonsilar plasma cells (n=5, TPC), Memory B cells (n=8, MB), Follicular lymphoma (n=77, FL) from independent specimens each. Star means p-value <= 0.05. Square dots are outliers (below 1st quartile or above 4th quartile). (**G**) As in panel F, expression values (FPKM) of JAG1 (upper panel) and JAG2 (bottom panel). (**H**) As in panel G, expression values (FPKM) of ADAM10 (upper panel) and ADAM 17 (bottom panel). (**I**) Flow cytometry to assess apoptosis of FL cell lines driven by DLL1 ligand. The % of apoptotic cells is observed on the upper-right quadrant of double positive labeled cells for propidium iodide (Y-axis) and Annexin V (X-axis) on DoHH2 (top) and Sc-1 (bottom) cell lines co-cultured with HS5-Control (right graph) or HS5-DLL1 (triplicates in left graphs) stromal cell line for 48h. See Supplementary Figure S5 for additional data.

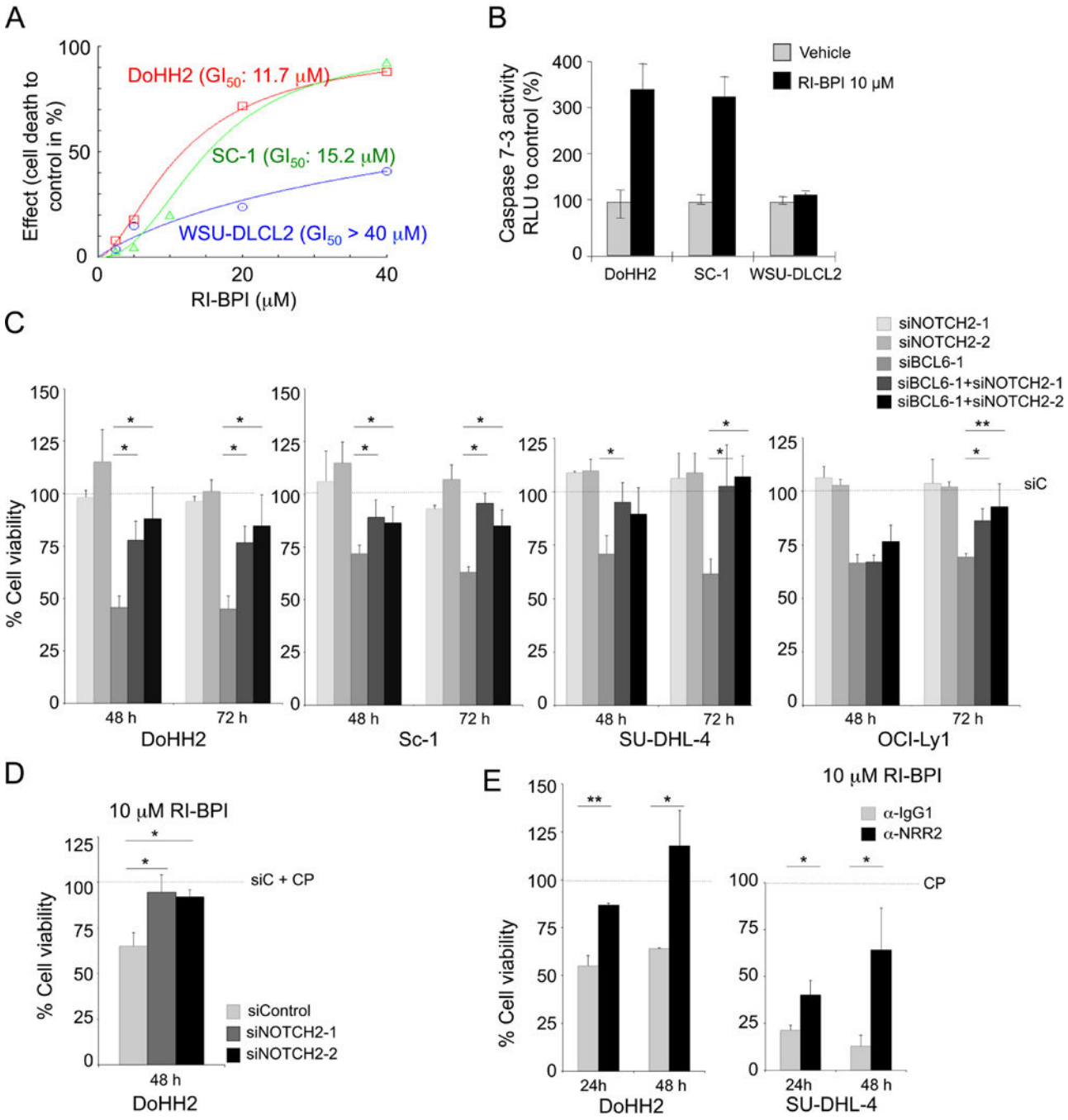

Figure 5. FL cells are dependent on BCL6 in a NOTCH2-dependent manner

(**A**) DoHH2, Sc-1 and WSU-DLCL2 FL cell lines were exposed to six concentrations of RI-BPI (from 1 to 40 μM) or vehicle (water) for 48 h. The X-axis shows the dose of RI-BPI. The Y-axis shows the fractional effect of RI-BPI vs. control on cell viability. The experiment was done in triplicates. The dose (in μM) that inhibited cell growth by 50% (GI_{50}) is shown next to each cell line. (**B**) Luminescent Caspase 7 and 3 activity assays were performed in FL cell lines (X-axis) exposed to vehicle (gray columns) or RI-BPI 10 μM (black columns) for 24 h. Results are expressed in percent of RLU to control (Y-axis). (**C**) DoHH2, Sc-1, SU-

DHL-4 and OCI-Ly1 cells were transfected *NOTCH2* siRNA, BCL6 siRNA or both as indicated and cell viability measured at 48 and 72 hours. The Y-axis represents percent cell viability, normalized to control siRNA (siC, dotted line). (**D**) DoHH2 cells were transfected with NOTCH2 siRNA as indicated and control siRNA as indicated, 24 hours post-transfection cells were treated with 10 μM RI-BPI and 24 hours post-treatment cell viability was measured as described before. The figure shows the mean of 3 experiments with SEM. (**E**) DoHH2 and SU-DHL-4 cells were pre-treated with anti-IgG1 or NOTCH2 antagonist antibody NRR2 for 24h and then exposed to 10 μM RI-BPI or control peptide (CP). Y-axis represents viability (At 24 and 48h) relative to control antibody (anti-IgG1) treated with CP. All experiments, unless otherwise indicated, were performed in triplicates and the error bars represent the SEM. Statistical significance is shown (p value one-tailed *t* test): * $p<0.05$; **$p<0.005$. See Supplementary Figures S6 and S7 for additional data.

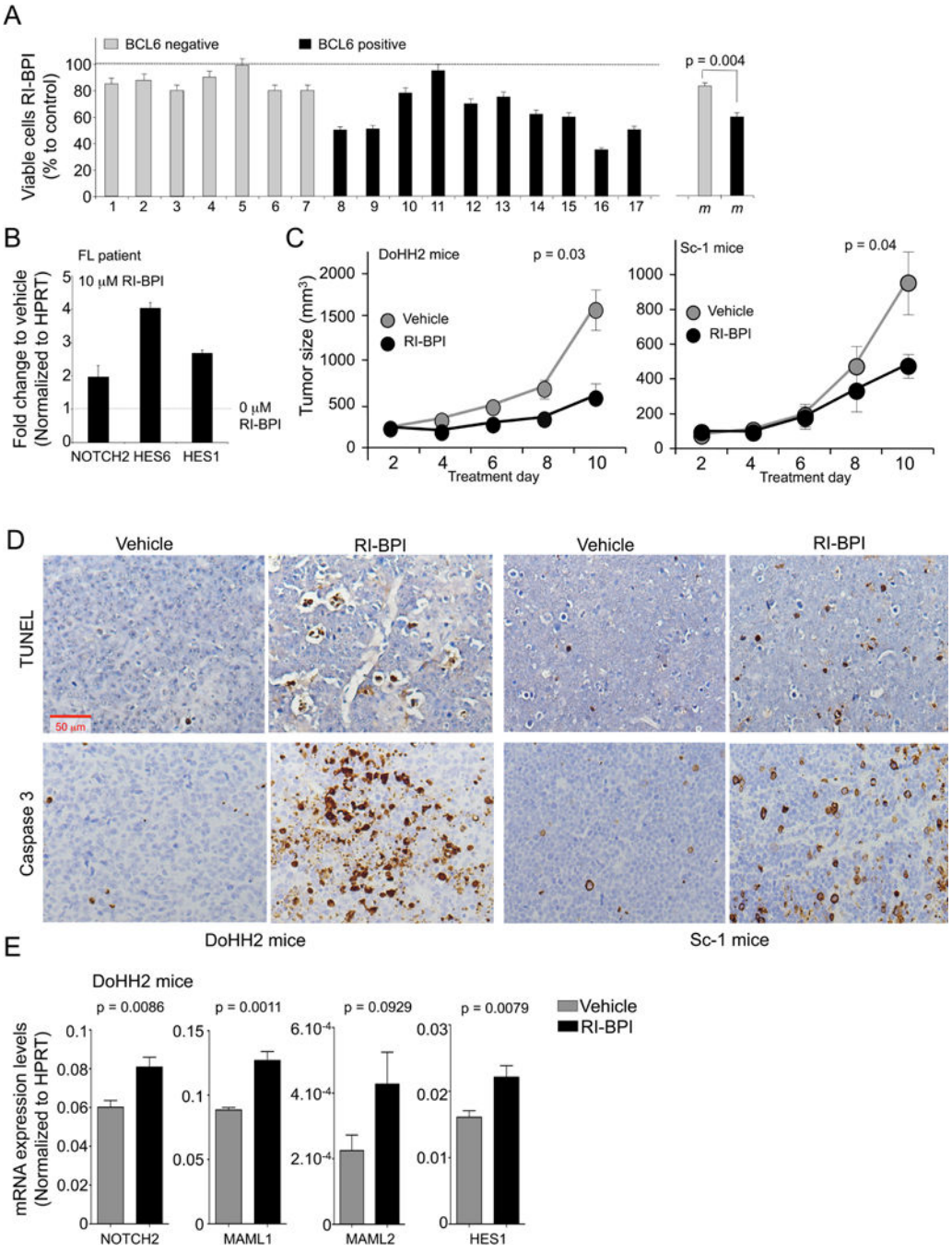

Figure 6. RI-BPI suppresses FL tumors *in vivo* and *ex vivo*

(**A**) Single cell suspensions of 17 confirmed FL specimens were exposed to vehicle (Control line) or 20 μM of RI-BPI (except case 14 that was treated with 5 μM) for 48 h. Seven samples were BCL6 negative (gray columns) and 10 samples were BCL6 positive (black columns). Cell viability (represented as percent of control treated cells) is shown on the Y-axis. Individual cases as well as the average for all the cases (m) are shown on the X-axis. Statistical significance (unpaired *t* test) was determined for the average of BCL6 positive vs. BCL6 negative cases. The experiment was carried out in duplicates. (**B**) An FL specimen

exposed to 10 μM RI-BPI was harvested 48h post-treatment and mRNA abundance examined by QPCR for *NOTCH2, HES6* and *HES1* and normalized to *HPRT*. Results are expressed as fold induction compared to control (vehicle). (**C**) Tumor growth plots in DoHH2 (left) and Sc-1 (right) xenografted mice treated with vehicle (PBS, n=5, gray lines) or RI-BPI 25 mg/kg/day (n=5, black lines) for 10 consecutive days. The Y-axis indicates tumor volume (in mm^3) and X-axis days of treatment. The p values represent the comparison of tumor volumes in treated to control mice at day 10 by Student's t test. (**D**) Representative immunohistochemistry images from DoHH2 and Sc-1 tumors after treatment with control or RI-BPI assayed for apoptosis by TUNEL and caspase 3 staining (top and bottom panels respectively). Red bar represents 50 μm. (**E**) QPCR was performed in triplicate from the DoHH2 FL xenografts of mice treated with vehicle (n=4) or RI-BPI 25 mg/kg/day for seven days (n=4) to assess transcript abundance of *NOTCH2, MAML1, MAML2 and HES1*, normalized to *HPRT*. Statistical significance was determined by Mann-Whitney test. See Supplementary Figure S8 for additional data.